

2012-8

Proximity Study of a UWB Directional Conformal Antenna on Water Pipe

Domenico Gaetano

Technological University Dublin

Max Ammann

Technological University Dublin, max.ammann@tudublin.ie

Patrick McEvoy

Technological University Dublin, patrick.mcevoy@tudublin.ie

See next page for additional authors

Follow this and additional works at: <https://arrow.tudublin.ie/ahfrcart>



Part of the [Systems and Communications Commons](#)

Recommended Citation

Gaetano, D. et al. (2012) Proximity Study of a UWB Directional Conformal Antenna on Water Pipe, *Microwave and Optical Technology Letters*, vol. 53, no. 8, pp. 1982-1986, 08/2012. doi10.1002/mop.26979

This Article is brought to you for free and open access by the Antenna & High Frequency Research Centre at ARROW@TU Dublin. It has been accepted for inclusion in Articles by an authorized administrator of ARROW@TU Dublin. For more information, please contact arrow.admin@tudublin.ie, aisling.coyne@tudublin.ie, vera.kilshaw@tudublin.ie.

Funder: SFI

Authors

Domenico Gaetano, Max Ammann, Patrick McEvoy, Matthias John, Louise Keating, and Frances Horgan

PROXIMITY STUDY OF A CONFORMAL UWB DIRECTIONAL ANTENNA ON WATER PIPE

Domenico Gaetano¹, Max J. Ammann¹, Patrick Mc Evoy¹, Matthias John², Louise Keating³, Frances Horgan³

¹Antenna & High Frequency Research Centre,
²The Telecommunications Research Centre (CTVR)
 Dublin Institute of Technology, Dublin 8, Ireland
 domenico.gaetano@student.dit.ie

³School of Physiotherapy, The Royal College of Surgeons
 in Ireland, 123 St. Stephens Green, Dublin 2, Ireland
 fhorgan@rcsi.ie

ABSTRACT: A preliminary study on the conformal properties of an antipodal exponentially tapered antenna placed on the surface of a flow meter system in the UWB range is presented. It was observed that the water effect can be mitigated by shifting the antenna away from the pipe surface.

Key words: Vivaldi; Conformal; Water Pipe; UWB.

1. Introduction

A small, flexible and low-profile antenna can permit an easy integration onto the curved surface of a circular cross-section pipe for communications between flow rate meter devices. An antipodal Vivaldi antenna provides a broadband, end-fire pattern and a large matched bandwidth. The effect of flexing the antenna substrate and the metallic elements is studied for bending around the principal axis. Although the conformal properties have been largely studied for resonant-type antennas [1], few investigations are reported on the performance of curved travelling wave antennas [2]. While conformal antennas were analyzed [3] in proximity to a water pipe, the aim of this paper is to mitigate the inefficiency introduced by the lossy materials by increasing the distance between antenna and pipe. The simulation results have been validated with prototypes.

2. Vivaldi Antenna

Figure 1a shows the geometry of the antipodal Vivaldi antenna [4-6], which is excited without a balun and fits on a compact substrate with dimensions 50×53 mm. The antenna flexibility is guaranteed by the thin 0.375 mm Duroid DT 5870 dielectric substrate ($\epsilon_r=2.33$, loss tangent = 0.0012). The antenna is designed with two exponentially tapered curves following the equations (1) (2), with the sides connected by a spline.

$$0.125 * e^{0.109t} \text{ for } 0 < t < 48.5 \text{ [mm]} \quad (1)$$

$$0.11 * e^{0.352t} \text{ for } 0 < t < 15 \text{ [mm]} \quad (2)$$

The antenna is optimized for UWB in terms of radiation patterns and matching for a free space environment in CST Microwave Studio [7].

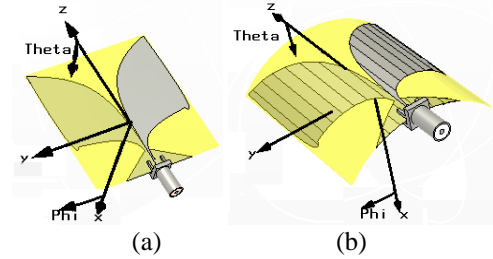


Figure 1 Antipodal Vivaldi Antenna in free space (a), conformal free space (b)

The back lobe radiation is reduced due to these spline shapes [4]. The geometry of the microstrip lines and the twin lines have been designed to guarantee an impedance as close as possible to 50 Ω in the intersection point [8, 9]. The simulation is in good agreement with measurement, as seen in Figure 2 and in Figure 3.

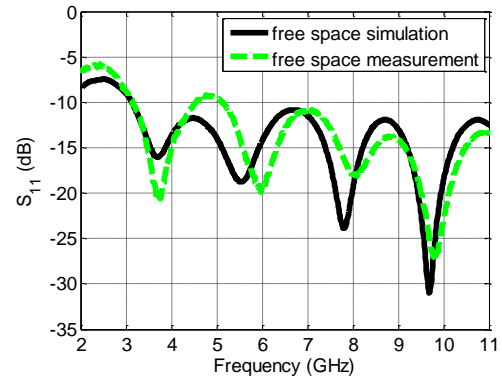


Figure 2 S_{11} of the simulated and measured planar antenna in free space.

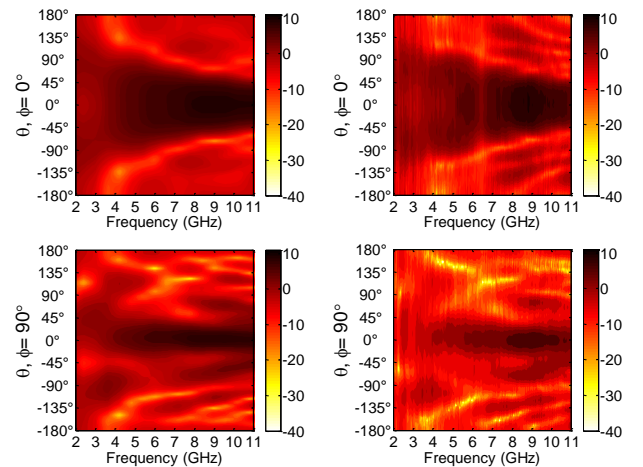


Figure 3 3-D radiation patterns (dBi) of the simulated (first column) and measured (second column) planar antenna in free space for $\phi = 0^\circ$ (first row) and $\phi = 90^\circ$ (second row).

3. Conformity and Water-Pipe effects

A section of PVC pipe ($\epsilon_r = 2.9$, loss tangent = 0.086 @ $f = 2$ GHz, 0.0182 @ $f = 11$ GHz) of diameter 56 mm, thickness 2.8 mm and length 58 cm was modeled. The antenna end-fire direction and the longitudinal pipe axis are aligned with the z-axis as shown in Figure 4.

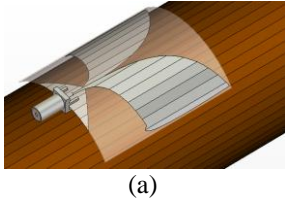


Figure 4 Antipodal Vivaldi antenna conformal.

Four different cases were considered: the planar antenna in free space shown in Figure 1a, the conformal-shaped antenna in free space shown in Figure 1b, the conformal-shaped antenna on an empty PVC pipe and finally, the conformal shaped antenna on a water ($\epsilon_r = 78$, $\sigma = 1.59$ S/m) filled pipe. The antenna cannot be completely attached to the pipe surface because the connector fringe overlaps with the pipe. For this reason a 3 mm Styrofoam layer has been added between the antenna and pipe. The comparison between simulation and measurement of the S_{11} for the four cases are shown in Figure 5.

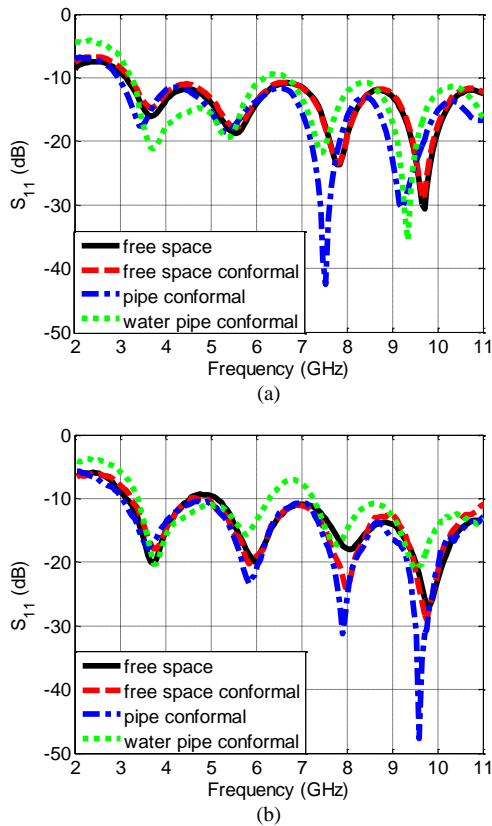


Figure 5 Simulated (a) and measured (b) S_{11} of free space antenna (black), conformal free space antenna (red), pipe conformal (blue) and pipe water conformal (green) .

There is good agreement between the simulated and measured S_{11} for the cases considered. The planar and the free space conformal antennas show a similar behavior, with a -10 dB bandwidth in all the UWB range. When the antenna is near to either the empty or water-filled pipe, the resonant frequencies shift due to dielectric loading, which increases the effective permittivity of the antenna. Figure 6 illustrates the radiation patterns of the measured antenna gain for $\phi = 0^\circ$ and $\phi = 90^\circ$.

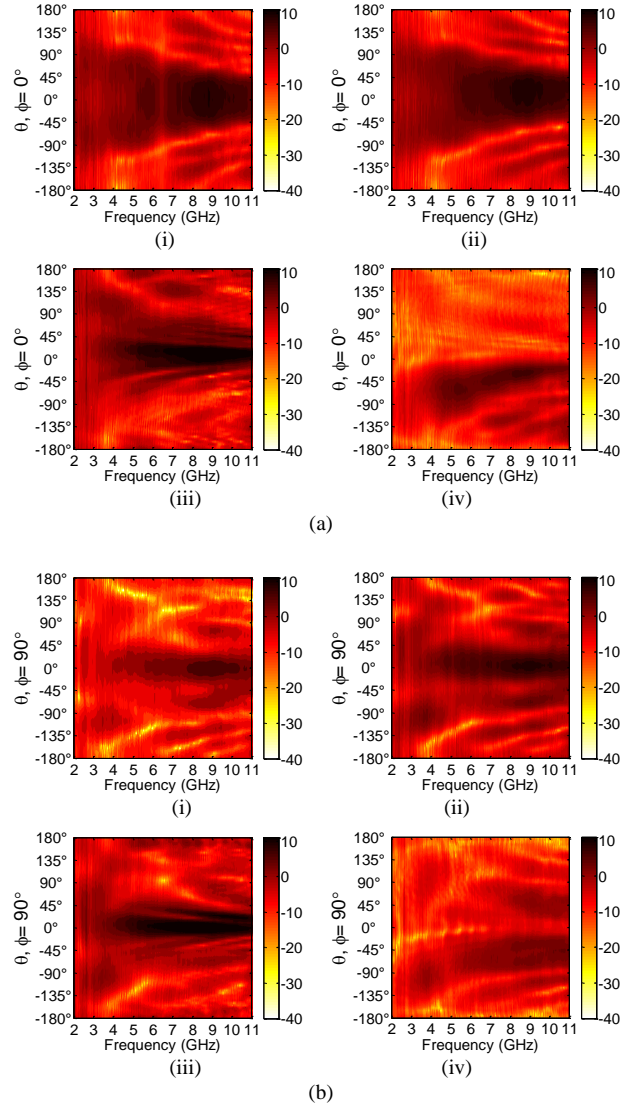


Figure 6 Measured 3-D radiation patterns (dBi) of the absolute gain for the free space antenna (i), conformal free space antenna (ii), pipe conformal (iii) and pipe water conformal (iv) for $\phi = 0^\circ$ (a) and for $\phi = 90^\circ$ (b).

The shape of the absolute gain remains the same when the antenna is curved, but the cross polarization is greater, the beamwidth is larger and the gain is slightly less. When the antenna is close to the pipe, the main beam is narrower and weaker. Finally, the presence of the water modified the shape of the main beam, now pointing in the $\theta < 0^\circ$ direction and further decreasing the antenna gain.

4. Pipe Proximity

The previous study [3] demonstrates an efficiency decrement when the antenna is close to the water pipe surface. This section is intended to study different proximity distances and characterize the water load on the antenna performance. The aim is to understand the optimum distance of the antenna from the pipe to maximize the absolute gain. Considering the z-axis oriented pipe, the parameter proximity is defined as the distance between the water surface and the antenna ground plane, as shown in Figure 7.

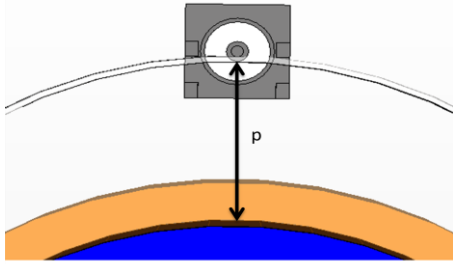


Figure 7 Description of the parameter proximity ($5.23 \text{ mm} \leq p \leq 18.23 \text{ mm}$).

Three separation distances have been studied: 5.23 mm, 7.23 mm and 18.23 mm. The measured S_{11} with different proximity variables are shown in Figure 8.

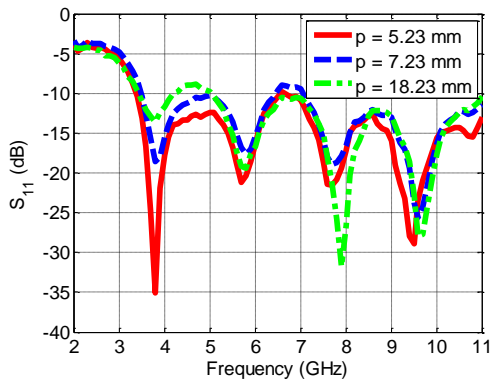


Figure 8 Measured S_{11} of water pipe conformal antipodal Vivaldi antenna with different proximity distances.

The S_{11} is slightly influenced by the presence of the water. Although the water is considerably lossy with high relative permittivity, the distance from the antenna limits its influence. As the distance between the antenna and the pipe increases, the loss decreases and the bandwidth decreases. In Figure 9 the radiation patterns are shown in function of the listed proximity variables for $\phi = 0^\circ$ and $\phi = 90^\circ$.

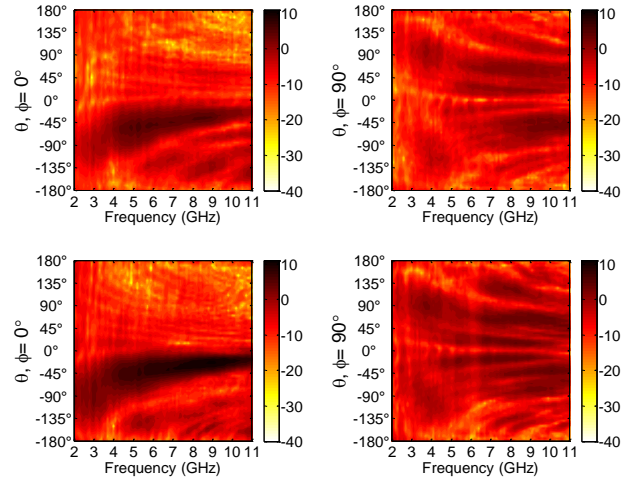
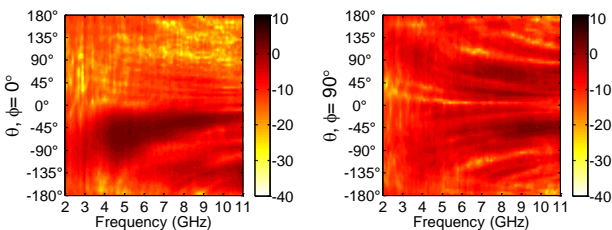


Figure 9 Measured 3-D radiation patterns (dBi) of the absolute gain for the water pipe conformal antenna for $\phi = 0^\circ$ (first column) and $\phi = 90^\circ$ (second column) and 5.23 mm (first row), 7.23 mm (second row) and 18.23 mm (third row) proximity.

The efficiency of the antenna depends on the proximity distance: when the antenna is closer to the pipe surface, the losses are greater and the gain is reduced. Although the gain is greater when the antenna is distant from the water pipe, due to the lower losses, the pattern shape is still influenced. The beam is reflected by the presence of the water, changing the angle of the main direction. Considering the $\phi = 0^\circ$ plane, the absolute gain relative to the direction below the antenna ($\theta > 0^\circ$) is low because the small transmitted component is attenuated by the water. The antenna has a good absolute gain in the direction above the antenna ($\theta < 0^\circ$). In particular the measured radiation patterns relative to the direction $\phi = 0^\circ$, $\theta = -30^\circ$ are shown in Figure 10.

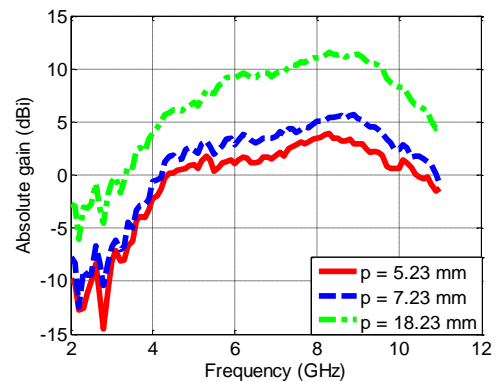


Figure 10 Measured radiation pattern for $\phi = 0^\circ$ and $\theta = -30^\circ$.

The gain becomes greater as the distance from the pipe surface increases. At some frequencies it is possible to have a value of gain greater than the free space case. The presence of the water reflects the incident wave, creating constructive and destructive interferences above the antenna and changes the patterns respect to the conformal free space case. Although there is an UWB band of frequencies where the antenna performance can be considered acceptable, the main direction is not end-fired, but tilted above the antenna. The whole system can be

considered as a dielectric interface, comprising free space and water, as shown in Figure 11.

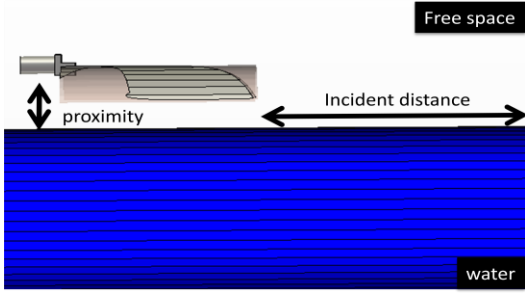


Figure 11 System description for the calculation of the reflection coefficient.

An incident wave propagates from the antenna to the water surface: part of the wave is reflected, another part is transmitted. The reflection coefficient has been calculated. The presence of the pipe is neglected, due to the low permittivity and losses. The mathematical formulas consider two different polarizations for the electric field as a function of the planar interface between the two dielectric regions. In this case the curved water surface is approximated by a planar surface parallel to the Y-Z plane below the antenna. The incident wave can be considered as a linear combination of two orthogonal polarizations. Considering two lossless regions at the interface, there are two different formulas [9] to calculate the parallel and perpendicular reflection coefficient:

$$\Gamma_{\parallel} = \frac{\eta_2 \cos \theta_t - \eta_0 \cos \theta_i}{\eta_2 \cos \theta_t + \eta_0 \cos \theta_i}, \quad (3)$$

$$\Gamma_{\perp} = \frac{\eta_2 \cos \theta_i - \eta_0 \cos \theta_t}{\eta_2 \cos \theta_i + \eta_0 \cos \theta_t}, \quad (4)$$

where:

- θ_t is the angle of the transmitted wave, equal to:

$$\theta_t = a \sin\left(\frac{k_1}{k_2} \sin(\theta_i)\right); \quad (5)$$

- η_0 is the free space impedance, equal to:

$$\eta_0 = \sqrt{\frac{\mu_0}{\epsilon_0}} = 120\pi; \quad (6)$$

- η_2 is the water impedance, equal to

$$\eta_2 = \frac{\eta_0}{\sqrt{\epsilon_2}}; \quad (7)$$

The calculated reflection coefficients are shown as a function of the incident distances, bound to the incident angle θ_i , in Figure 12. The reflection coefficient behavior is different for the two polarizations:

- In the parallel polarization case, the reflection coefficient Γ is very low for small distances, and converges to 0.8 for infinity.

- In the perpendicular polarization case, the reflection coefficient Γ is approximately 1 for small distances, and converges to 0.8 for infinity.

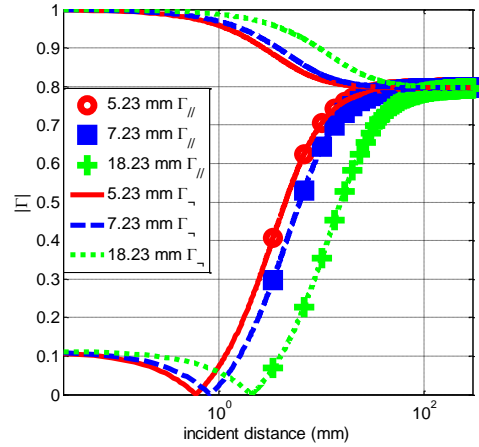


Figure 12 Calculated reflection coefficient for different proximity distances (logarithmic scale).

The convergence of the reflection coefficient is fast and 80% of the incident wave is reflected by the water for almost all the incident distances. Moreover, the perpendicular component of the reflection coefficient is predominant.

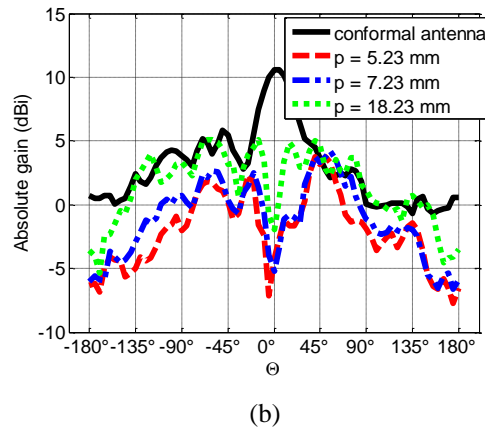
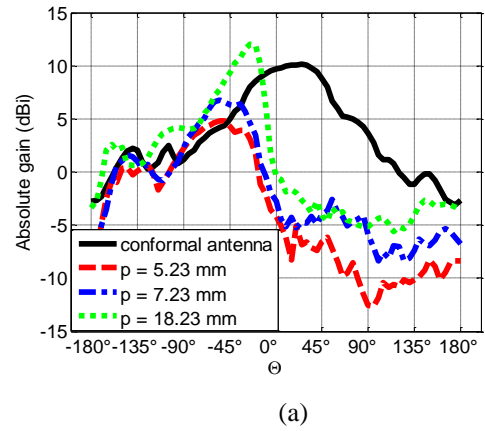


Figure 13 Maximum gain as a function of the angle for $\varphi = 0^\circ$ (a) and $\varphi = 90^\circ$ (b).

Considering the maximum gain values over the frequency band for each direction, a comparison between the conformal free space and the water-pipe cases are shown in Figure 13 for $\varphi = 0^\circ$ and $\varphi = 90^\circ$ planes. Considering the $\varphi = 0^\circ$ case, it is evident that for θ values below 0° the gain of the water pipe loaded Vivaldi antenna is greater than the conformal free space case, due to the added component of the reflected waves. The increment is greater for the 13 mm case, while it is visible for few angle intervals for smaller proximity distances cases. The smaller values of gain for θ angles above 0° is due to the high water attenuation on the partially transmitted wave. There is no gain increment in the $\varphi = 90^\circ$ plane, because there are no reflection contributions.

5. Conclusion

The conformal shaping increases the cross polarization, independent of the bend plane. The water-pipe presence significantly influences the performance of the antenna by adding further material losses. This can be mitigated by maintaining some minimal surface distance from the pipe, although the radiation pattern shape is not improved. Besides it is calculated that 80% of the radiated wave is reflected by the water inside the pipe causing many changes in the radiation pattern shape. The radiation pattern main direction is no longer a function of the lossy material located in the near field, but depends on the reflection behavior in the far field.

6. Acknowledgements

This publication has emanated from research conducted with the financial support of Science Foundation Ireland under Grant Number 09/IN.1/I2652.

References

- [1] Q. Bai and R. Langley, Crumpled textile antennas, *Electronics Letters* 45 (2009), 436-438.
- [2] N. Symeon, G. E. Ponchak, J. Papapolymerou and M. M. Tentzeris, Conformal double exponentially tapered slot antenna (DE TSA) on LCP for UWB applications, *Trans Antennas and Propag* 54 (2006), 1663-1669.
- [3] D. Gaetano, M. J. Ammann, P. McEvoy, M. John, L. Keating and F. Horgan, A conformal UWB directional antenna, *EUCAP* (2011), 1113-1116.
- [4] E. Gazit, Improved design of the Vivaldi antenna, *Microw Antennas and Propag* 135 (1988), 89-92.
- [5] C. Zhi Ning, M. J. Ammann, Q. Xianming, W. Xuan Hui, T. S. P. See and A. Cat, Planar antennas, *Microwave Magazine* 7 (2006), 63-73.
- [6] M. John, M. J. Ammann and P. McEvoy, UWB Vivaldi antenna based on a spline geometry with frequency band-notch, *Antennas and Propag Society International Symposium* (2008), 1-4.
- [7] Microwave Studio, Computer Simulation Technology, <http://www.cst.de>.
- [8] Z. Xiaodong, A. Yarovoy and L. P. Ligthart, Circularly tapered antipodal vivaldi antenna for array-based ultra-wideband near-field imaging, *EuRAD* (2009), 250-253.
- [9] K. C. Gupta, R. Garg, I. Bahl and P. Bhartia, *Microstrip lines and slotlines*, Artech House, Boston, 1996.
- [10] D. M. Pozar, *Microwave engineering*, Wiley, New York, 1998.